Mem. Descr. Carta Geol. d'It.
LXII (2003), pp. 55-74
16 figg.

Wide-angle Sea-Land connections as an integration of the CROP MARE II project

Connessione mare-terra realizzate dal gruppo Sea-Land come integrazione del progetto CROP MARE II

CAIELLI G. ([1]), CAPIZZI P. ([2]), CORSI A. ([1]), DE FRANCO R. ([1]), LUZIO D. ([2]), DE LUCA L. ([2]), VITALE M. ([2])

ABSTRACT - A report is given of the activity of the Sea Land Group[(a)] concerning the CROP MARE II seismic project.

In this experiment, jointly with near-vertical seismic data acquisition (NVR), the Sea Land Group acquired high-density wide-angle reflection/refraction data (WARR) in some off-shore/on-shore configurations along the Italian coast.

A concise and complete overview is given of the acquisition scheme, the processing techniques used and the problems connected with the acquisition and management of this kind of data.

Our experience led us to get over the standard processing techniques commonly adopted in WARR and NVR seismics, setting up innovative Matlab procedures for data processing. Such a development was directed at an integrated use of small- and great-offset seismic signals for the optimisation of imaging and modelling of lithospheric structures.

KEY WORDS: WARR seismics, seismic processing, seismic imaging, geophysical modelling.

RIASSUNTO - In questo contributo è descritta l'esperienza del Gruppo Sea Land che si è costituito per operare nell'ambito del progetto CROP MARE II di sismica crostale.

Durante questo progetto sono stati registrati, contemporaneamente ai dati a riflessione quasi verticale (NVR), dati a rifrazione e riflessione a grande angolo (WARR) ad elevata densità mediante configurazioni terra/mare dei profili ubicati attorno la costa italiana.

Questo lavoro fornisce una descrizione completa della procedura di acquisizione e dei problemi ad essa connessi e degli schemi di processamento che sono stati applicati ai dati.

Questa esperienza ha consentito di superare le tecniche standard di elaborazione generalmente applicate ai dati WARR e NVR e di realizzare in ambiente Matlab procedure software innovative per l'elaborazione dei dati sismici. Tale sviluppo è stato orientato verso l'uso integrato di segnali sismici a piccolo e grande angolo per l'ottimizzazione dell'imaging e della modellazione di strutture litosferiche.

PAROLE CHIAVE: Sismica a grande angolo, processing sismico, imaging sismico, modelli geofisici.

([1]) Institute for the Dynamics of Environmental Processes - CNR, Milan, Italy
([2]) Dep. of Chemistry and Physics of the Earth (C.F.T.A.), Palermo University, Italy
([a]) Research units of the Sea Land Group: Cosenza (University - supervisor I. Guerra); Milan (CNR- supervisor G. Biella); Milan (University – supervisor R. Cassinis); Naples (INGV – supervisor G. Gaudiosi); Palermo (University - supervisor D. Luzio)

1. - INTRODUCTION

In recent years, many international projects for the investigation of lithospheric structures have included the acquisition of both small- and great-offset seismic data. The experiments of major scientific relevance conducted until 1986 are enumerated in MOONEY & BROCHER (1987) and an overview of many similar experiments performed more recently is reported in CASSINIS & LOZEJ (2000).

The advantages of combined reflection/refraction studies have been described in BERRY & MAIR (1980), MEISSNER *et alii* (1983), and BRAILE & CHIANG (1986).

Wide-angle reflection/refraction data acquisition provides an economic means to complement the information obtained from the near-vertical reflection technique on the Earth's lithosphere structure.

In particular, the inversion of WARR data could be constrained with the near-surface velocity analysis and boundary geometries coming from the interpretation of NVR profiles. This latter on its turn could be improved using the velocity functions deduced by WARR modelling, in order to produce, e.g., a better stack and migration of data. Generally speaking, near-vertical reflection (NVR) and wide-angle reflection/refraction (WARR) data should be processed and interpreted by procedures co-operatively interacting in many steps, such as to optimise the choice of NVR processing parameters using preliminary results of WARR data imaging and modelling, and to refine the model design through the constraints set by the improved seismic sections.

The contributions summarised in this paper derive from a joint experience of the researchers and operators of the Sea Land Group, who have been working in these years on different aspects connected with the analysis of wide-angle data, in the frame of the CROP MARE II project. In particular, a short but complete overview of the innovative procedures developed will be given and the problems connected with WARR marine data processing will be discussed.

2. - DATA ACQUISITION

The necessary conditions to obtain good-quality refracted and reflected arrivals from the crust and upper mantle up to very large offsets are a powerful airgun source, low environmental noise in the recording sites and the correct suppression of static shifts.

It has been verified in many international projects that, using multichannel recording and performing the stacking of adjacent records, seismic signals relative to powerful airgun arrays can be detected up to offsets of 700 km (BABEL WORKING GROUP, 1991), while signals from a relatively small airgun source could be recorded beyond 200 km (JOKAT & FLUEH, 1987 and LUND *et alii*, 1987). In some recent projects, airgun arrays operating in single-bubble mode have been adopted in order to increase the investigation depth (HIRN *et alii*, 1997; MJELDE *et alii*, 1997; PETRONIO & CERNOBORI, 2000).

In the CROP MARE II project a 32-Bolt airgun of 90 l (M/N EXPLORA - OGS) was used.

The decision to integrate the CROP MARE II experiment with the acquisition of the wide-angle data was based on the results of a previous experience of the Institute of Geophysics of Genoa (AUGLIERA *et alii*, 1992), even though the source parameters employed were not optimised for wide-angle data recording. This strongly affected the quality of the signals recorded.

The shooting interval generally adopted in the offshore seismic profile (20 s, corresponding to a trace spacing of about 50 m) produced a wraparound noise in the wide-angle data. This effect occurs at the offsets for which slow phases, typically water waves, arrive to the recording station with travel times greater than the interval between consecutive shots. An example of this is shown in figure 1, which represents a portion of a CROP MARE II section where the arrivals relative to the water wave can be observed.

For a shooting interval of 20 s, the arrival of the water wave produced by a shot returns as a disturbance effect in the lower part of the seismic section at an offset about 30 km, where it interferes with the body-waves produced by the next shot. In order to avoid the wraparound effect, larger shooting intervals (120 s) were used in the Antarctic TENAP project (DELLA VEDOVA *et alii,* 1997). This effect was avoided in CROP MARE II lines M13 and M14 (GRUPPO SEA LAND CROP MARE II, 1994), the only two lines of this project which had been recorded without towed cable, using the same airgun array but shot intervals of 60 s (corresponding to a trace interval of about 150 m).

The choice of the shooting parameters should also take into account that decreasing the inter-distance between shots would decrease spatial aliasing and using a variable shooting time interval would limit the applicability of standard algorithms for 2D filtering (PETRONIO, 1997).

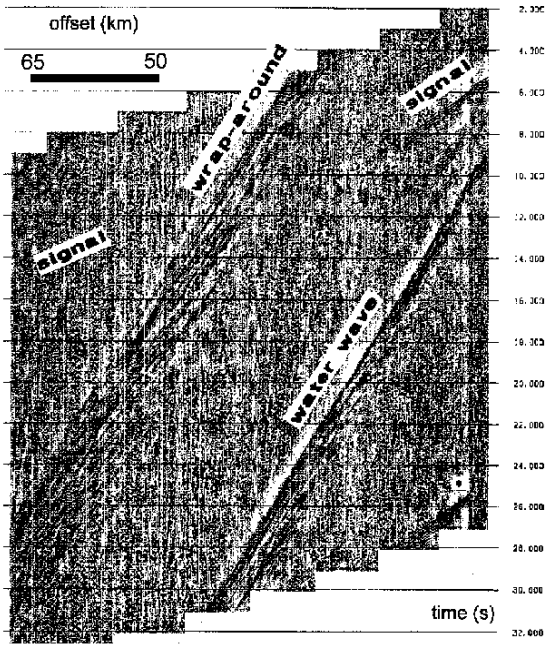

Fig. 1 - A portion of a CROP MARE II M25 seismic section in which the arrivals relative to the water wave can be observed.

- Una porzione della sezione sismica CROP MARE II M25 in cui si possono osservare gli arrivi relativi all'onda che si propaga in acqua.

Each airgun line was recorded by mobile seismic stations equipped with a single 3-component 1 Hz geophone recording system. Because of the limited budget available, only 15 mobile inland stations were used during the whole survey; in particular, each seismic line was recorded on average by 2.9 stations.

The recording stations were generally placed nearly to each other along the on-shore extension of the NVR profiles and seldom in a fan configuration with respect to the profiles themselves (fig. 2). The profile acquisition geometry was considered more suitable for constructing 2D crustal velocity models, whilst the fan configuration could provide a more detailed imaging of the topography of a reflecting boundary. The acquisition parameters relative to each profile are reported in Table 1.

In some of the recording sites, two or more seismic stations were placed with a reciprocal distance between 50 m and 100 m in order to improve the signal-to-noise ratio by stacking the acquired signals.

The location of the recording sites was decided on those geological structures assumed a priori suitable for the acquisition of good-quality signals, on the basis of the comparison between the environmental noise levels recorded in different sites.

The receivers were generally placed on hard rock in order to achieve a probable high Q for the underlying medium.

Since most of the energy of airgun signals is in the frequency range 4-20 Hz, the data recording was carried out with sampling rate 62.5 Hz or 125 Hz; anti-aliasing filters with cut-off frequency equal respectively to 25 Hz or 50 Hz were applied.

Because of the low signal-to-noise ratio, it was very useful to employ digital stations with a high dynamic range, using oversampling and then decimation in the A/D conversion.

The shot-breaks were monitored on board by a radio-controlled time DCF and/or GPS, and the land stations were synchronised with the same time signal codes.

A total of about 3.0 Gb of digital signals was collected during approximately 1000 recording hours. Fifty people were engaged during the whole period for the selection of the recording sites and for the control of the mobile seismic stations.

A data compilation containing the original, standard- and advanced processed three-component seismic sections will be available on the FTP site idpa.cnr.it in the directory "cropmareatlas", together with lay-out, recording and processing parameters.

A preliminary version consisted in the publication by some Sea Land Group researchers of an atlas containing all original and standard-processed seismic sections relative to the vertical component. In this version the acquisition of the seismic lines of the French-Italian project Lisa (Mauffret, 1995; De Franco *et alii*, 1997) was also reported.

3. - DATA PROCESSING

As a consequence of the wide-angle data acquisition technique, the first step of the processing sequence is the conversion of a unique time series into a common-receiver gather.

Even though data processing packages produced by commercial groups for the analysis of NVR or very shallow refraction seismic data could have been applied to WARR data, some peculiarities present in these latter suggested designing a new software for pre-processing, signal enhancement and off-line and fan-profile processing, allowing both to achieve considerably improved Matlab processing algorithms and to use common PC's to execute the heavy calculations required by so large data matrices.

3.1. - Construction of data matrix

In the first stage, the data recorded blockwise in a format typical of the acquisition instrument are converted into one or more other formats compatible with the most widespread processing software

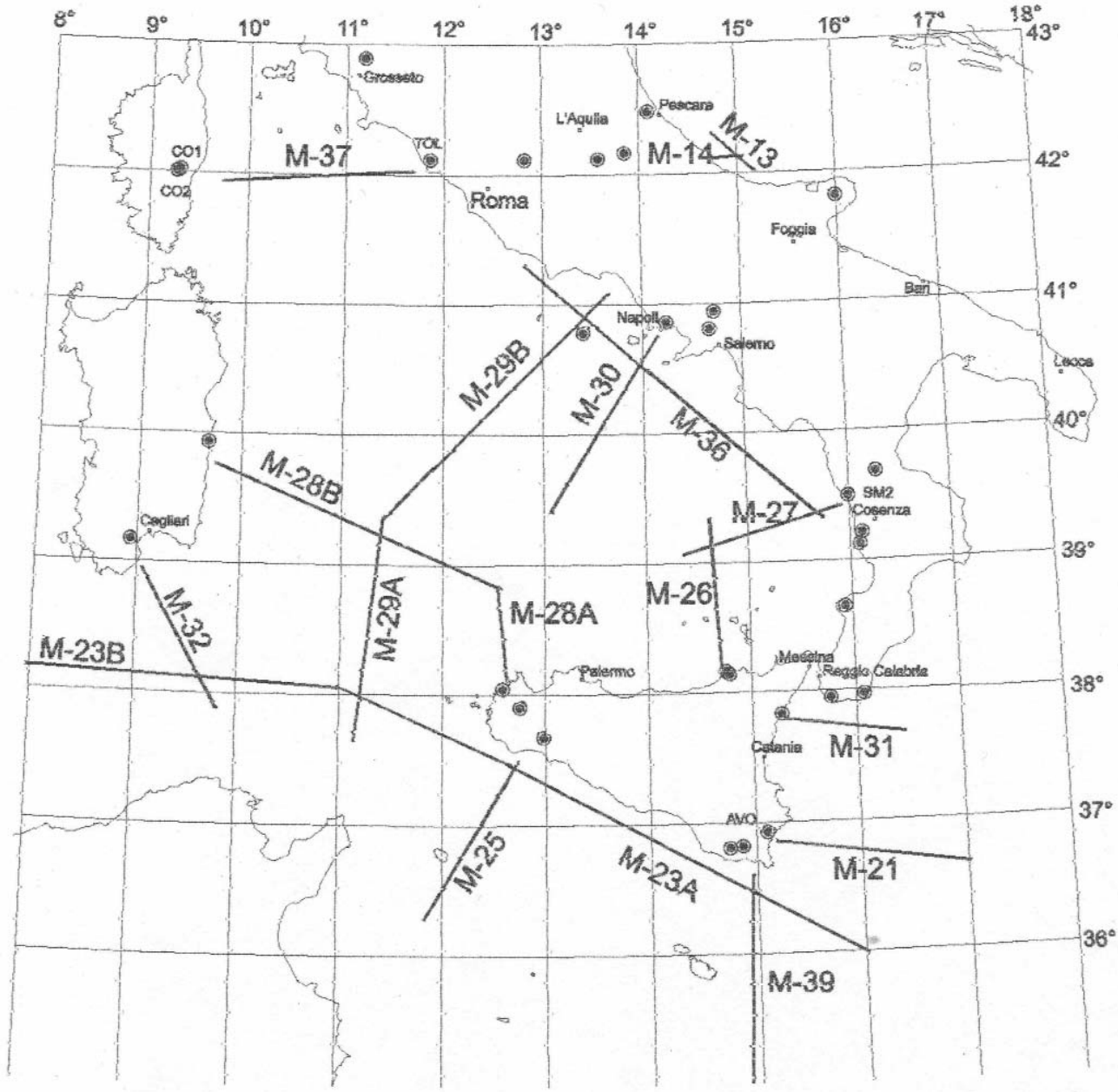

Fig. 2 - Location of the wide-angle seismic profiles recorded in the frame of the CROP MARE II Project.
- Ubicazione dei profili sismici a grande angolo acquisiti nell'ambito del Progetto CROP MARE II.

and stored once they have been collected into a unique time sequence.

In the second stage, a matrix is set up by rearranging the time sequence on the basis of the information about shooting time, receiver and shot co-ordinates and seafloor depth, which had been stored in a separate file. Such information constitutes the trace headers attributed each to a matrix column.

The number of rows (trace length) may be fixed a priori according to the investigation objectives. Each row is associated to a constant reduced time $t - x/v$, where t is the time elapsed after each shot, x the offset relative to each shot and v a reduction velocity.

The number of columns corresponds to the number of shots. Each column is associated to an abscissa which may represent an offset in the case of profile configuration, an azimuth in the case of fan configuration. In this case the azimuth is the clockwise angle between the north and the line orientated from the receiving station to the shot.

Tabella 1 - *Parametri di acquisizione dei dati dei singoli profili* – Parameters of data acquisition for each profile

Line	Station name	Station coordinates		Station elevation (m)	Maximum offset (km)	n. traces	Shooting intertime (s)	Sampling frequency (Hz)
M13	Maielletta	42°10.77'	14°6.47'	1560	79.816	106	60	62.5
	Sirente	42°7.68'	13°34.68'	1590	123.484	122	60	62.5
	Gargano	41°82'	15°99'	794	105.6	118	60	62.5
M14	Maielletta	42°18'	14°11'	1560	101.951	277	60	62.5
	Sirente	42°7.68'	13°34.68'	1590	132.465	277	60	62.5
	Gargano	41°49.17'	15°59.57'	794	114.319	275	60	62.5
M21	Avola	36°55.47'	15°5.7'	244	115.997	1832	20	62.5
	Avola	36°55.47'	15°5.7'	244	115.997	1832	20	62.5
	Pentedattilo	37°57.21'	15°45.69'	350			20	125
M23a	C.zzo Grande	36°48.53'	14°38.33'	125	163.27	1492	20	62.5
	Cave d'Ispica	36°49.78'	14°52.13'	280	163.27	1492	20	62.5
M23b	M. Magaggiaro	37°40.47'	12°59.03'	408	180.68	2952	20	62.5
	M.gna Grande	37°54.52'	12°45.07'	350	180.68	2952	20	62.5
M25	M. Magaggiaro	37°40.47'	12°59.03'	408	184.466	2870	20	62.5
	M.gna Grande	37°54.52'	12°45.07'	350	184.466	2870	20	62.5
M26	Brolo	38°8.75'	14°47.78'	370	132.218	1086	40	125
	Brolo	38°8.75'	14°47.78'	370	132.218	1086	40	125
	Capo d'Orlando	38°9.55'	14°44.97'	150	80.983	646	40	125
	Monte Cocuzzo	39°13.1'	16°8.02'	1535			40	125
	Drapia	38°38.91'	15°55.92'	450			40	125
M27	S. Martino	39°29.17'	16°6.55'	615	135.367	1079	40	125
	Spezzano	39°40.97'	16°17.18'	200	162.964	1033	40	125
	Aiello Calabro	39°7.26'	16°9.86'	417	152.21	914	40	125
M28a	Erice	38°3.6'	12°35.43'	280	85.896	1416	20	62.5
	Erice	38°3.6'	12°35.43'	280	85.896	1416	20	62.5
M28b	Arbatax	39°55.83'	9°40.78'	5	76.282	949	20	62.5
M29b	Ventotene	40°47.55'	13°25.71'	50	42.723	703	20	125
M30	Capodimonte	40°51.82'	14°14.39'	300	84.535	632	20	125
	Monte Vergine	40°56.17	14°43.73'	1260	123.71	1290	20	125
	Vesuvio Osservatorio Vesuviano	40°81' 40°48.6'	14°42' 14°11.49'	600 250	87.547	723	20 20	125 125
M31	Roccalumera	37°59.58'	15°22.13'	275	117.463	1707	20	62.5
	Roccalumera	37°59.58'	15°22.13'	275	117.463	1707	20	62.5
	Brancaleone	37°58.61'	16°4.28'	600	70.574	1665	20	125
	Brancaleone	37°58.61'	16°4.28'	600	70.574	1665	20	125
	Pentedattilo	37°57.21'	15°45.69'	350	66.32	1690	20	125
	Villagonia	37°50'	15°17.52'	50	70.574	1665	20	125
M32	Cagliari	39°9.95'	8°55.78'	310	127.035	1785	20	62.5
M36	Ventotene	40°47.55'	13°25.71'	50	77.018	1091	20	125
	Monte Vergine	40°94.0'	14°73'	1260	115.449	1371	20	125
	S. Giovanni a Piro	40°2.75'	15°27.83'	600	111.589	776	20	125
	San Martino	39°29.17'	16°6.65'	615	118.132	1602	20	125
M37	Tolfa	42°7.65'	11°51.45'	890	121.202	660	20	62.5
	Monte Flavio	42°7.27'	12°50.08'	840	201.951	1965	20	62.5
	Sirente	42°7.68'	13°34.68'	1590	192.256	686	20	62.5
	Montorsaio	42°53.72'	11°11.25'	400	105.355	751	20	62.5
	Corsica	42°1.02'	9°16.06'	700	203.644	1379	20	62.5
M39	Cave d'Ispica	36°49.78'	14°52.13'	280	147.285	2239	20	125
	Cave d'Ispica	36°49.78'	14°52.13'	280	147.285	2239	20	125

The choice between the two geometric configurations is made on the basis of azimuth and offset variations. A fan configuration is selected by default if the greatest azimuth difference is over 15° and the maximum offset increment is smaller than $1.4D_m$ (where D_m is the minimum shot-receiver distance), otherwise a profile configuration is chosen.

Since all offset and azimuth values are available from the header matrix, it is possible to switch from one configuration to the other at any time.

3.2. - Static correction

They can include corrections for the effect of source, receiver and seafloor level, as well as of the shallow sediment thickness.

The corrections carried out in the first processing stage were aimed at smoothing the phase correlation line observable on the seismic sections, in order to increase the efficiency of the de-noising algorithms generally based on stacking and correlation analysis along the profile.

Along each recorded profile the seafloor topography was reconstructed by SONAR pulses. By the bathymetric function $h(x)$, with x denoting the abscissa along the profile, and an apparent velocity vs. offset function $v_a(x)$, estimated for the first arrivals relative to an average crustal structure, a static correction in time and position was calculated for each trace of the seismic sections using the formula

$$s^c_{x'}(t') = s_x(t), \tag{2}$$

in which

$$t' = t - \frac{h(x)}{v_m} + \frac{h(x)v_a(x)}{v_s\sqrt{v_a^2(x) - v_s^2}},$$

$$x' = x + \frac{h(x)v_s}{\sqrt{v_a^2(x) - v_s^2}} - \frac{h(x)v_m}{\sqrt{v_a^2(x) - v_m^2}}, \tag{2}$$

The time and space corrections simulate the substitution of the water layer of velocity v_m with one whose velocity v_s approaches that of seafloor sedimentary layers, under the assumption that the ray emerges vertically in the water layer and with an emersion angle compatible with $v_a(x)$ in the substitute layer.

An application of the correction to a piece of the M25 CROP MARE II seismic section is shown in figure 3.

After de-noising, an inverse correction with respect to (1)-(2) is applied to the seismic sections so as to carry out the ray-tracing by resuming the correct velocity contrasts between the structures reconstructed in the modelling stage.

The static correction for local structures effects, such as those produced by small sedimentary basins, can be applied during the data interpretation to describe geometric and physical features of small-scale structures. Such corrections should be made by considering the information on the shapes of sedimentary-layer boundaries coming from the interpretation of NVR profiles recorded along the same line and other geological evidences when available.

3.3. - Amplitude balancing function

Mean and instantaneous automatic gain control (AGC) and an amplitude balancing function whose temporal trend is offset dependent can be applied to recover the amplitude decay effects. The latter is calculated as

$$A_i^c = A_i\left(t_i + t_0(x)\right)^{\alpha}, \tag{3}$$

where A_i and t_i are the amplitude and the positive reduced time of the i-th sample respectively, α is a positive exponent expressing the rate of the logarithm amplitude gain vs. the logarithm of a reduced time properly corrected and $t_0(x)$ is the correction function which depends on the offset according to some chosen criterion.

If $t_0(x) = x/v_r$, where v_r is the reduction velocity, the same gain will be applied to samples of equal non-reduced time belonging to different traces. In order to keep the ratio between the gains of the first and the last sample of each trace of a seismic section equal to k^{α}, the function

$$t_0(x) = \frac{\Delta t}{k-1} - \frac{x}{v_r}, \tag{4}$$

must be used in eq. (3), with Δt being the length of each trace.

The results of the application of a few amplitude recovery functions to a seismic fan are shown in figure 4.

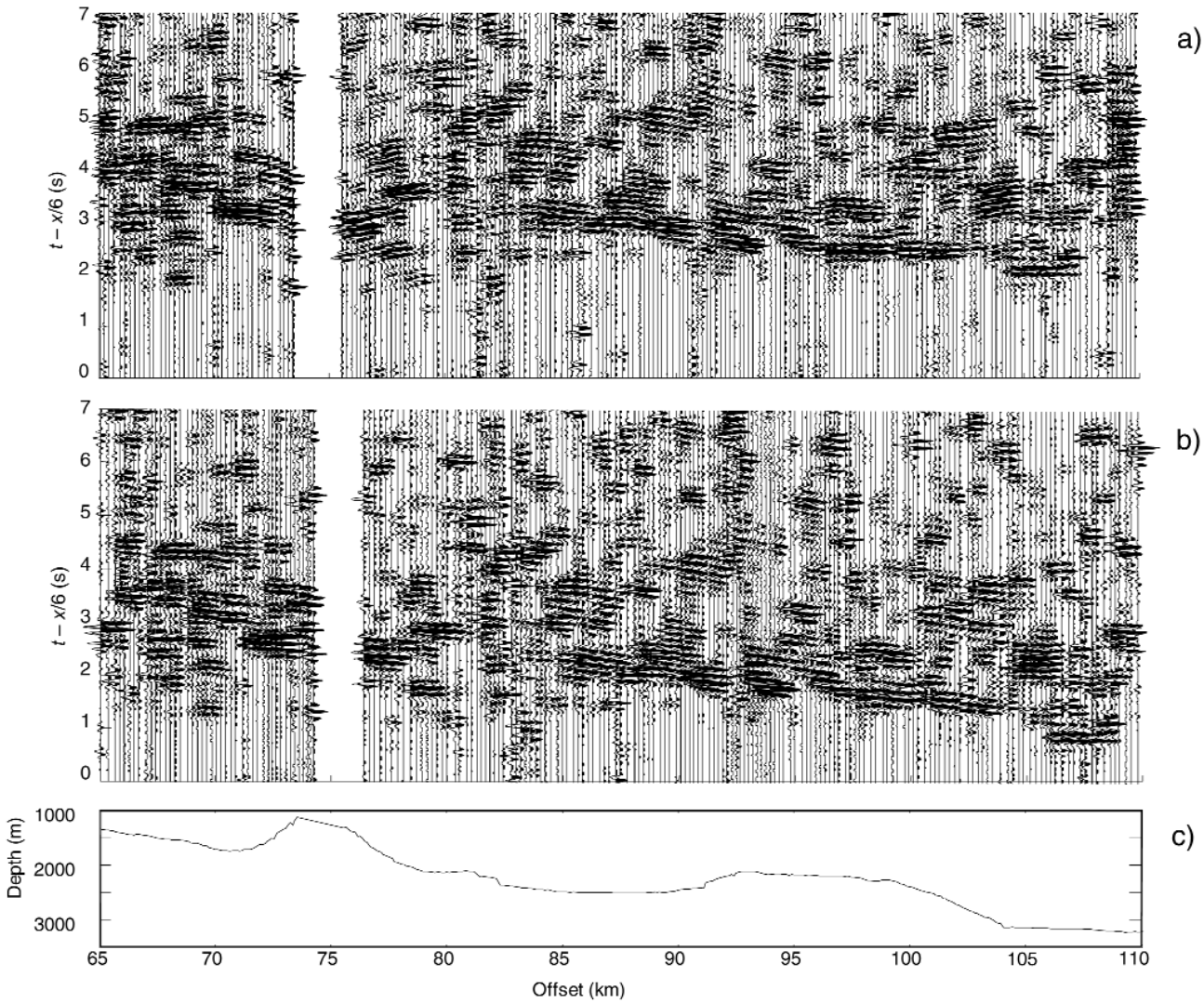

Fig. 3 - Effect of seafloor-level correction on a piece of the CROP MARE II M25 section: (a) original data; (b) corrected data; (c) seafloor profile. *- Effetto della correzione per l'effetto del fondo del mare su una porzione della sezione sismica CROP MARE II M25: (a) dati originali; (b) dati corretti; (c) batimetria.*

3.4. - Spectral analisis and 1D and 2D frequency-domain filtering

In order to better identify the noise and signal typical frequency ranges, average power spectra were estimated from the normalised spectra of a number of consecutive traces. Most of the energy relative to the signal present in the whole data set lies on average in the frequency range 4-18 Hz.

1D band-pass frequency filtering was carried out in several steps of the processing sequence. Often, a band-pass Butterworth filter in the range stated above and section from 3 to 7 was applied at the beginning of data processing to remove very low- and high-frequency noise.

Since the characteristics of noise and signal spectra can sensibly change as a function of offset and seismic-phase nature, better results can be obtained by using offset- and/or time-variant filters which allow to preserve the high-frequency content of shallower phases, and so increase the resolution in the shallower part of models. They prove particularly useful in the processing of long-recording data (over 20 s), as in the S-phase study by three-component data.

Sometimes, algorithms known as soft-thresholding filters, based on traces wavelet transform and thresholding of the obtained spectral coefficients (Donoho & Johnstone, 1994; Donoho, 1995), were applied to increase the signal-to-noise ratio. They consist in an approximated signal reconstruction, by inverse wavelet transform, of the coefficients filtered by setting to zero those with absolute values lower than $\eta = \sigma\sqrt{2\log m}$ and shifting the others towards zero by this quantity, m being the number of samples

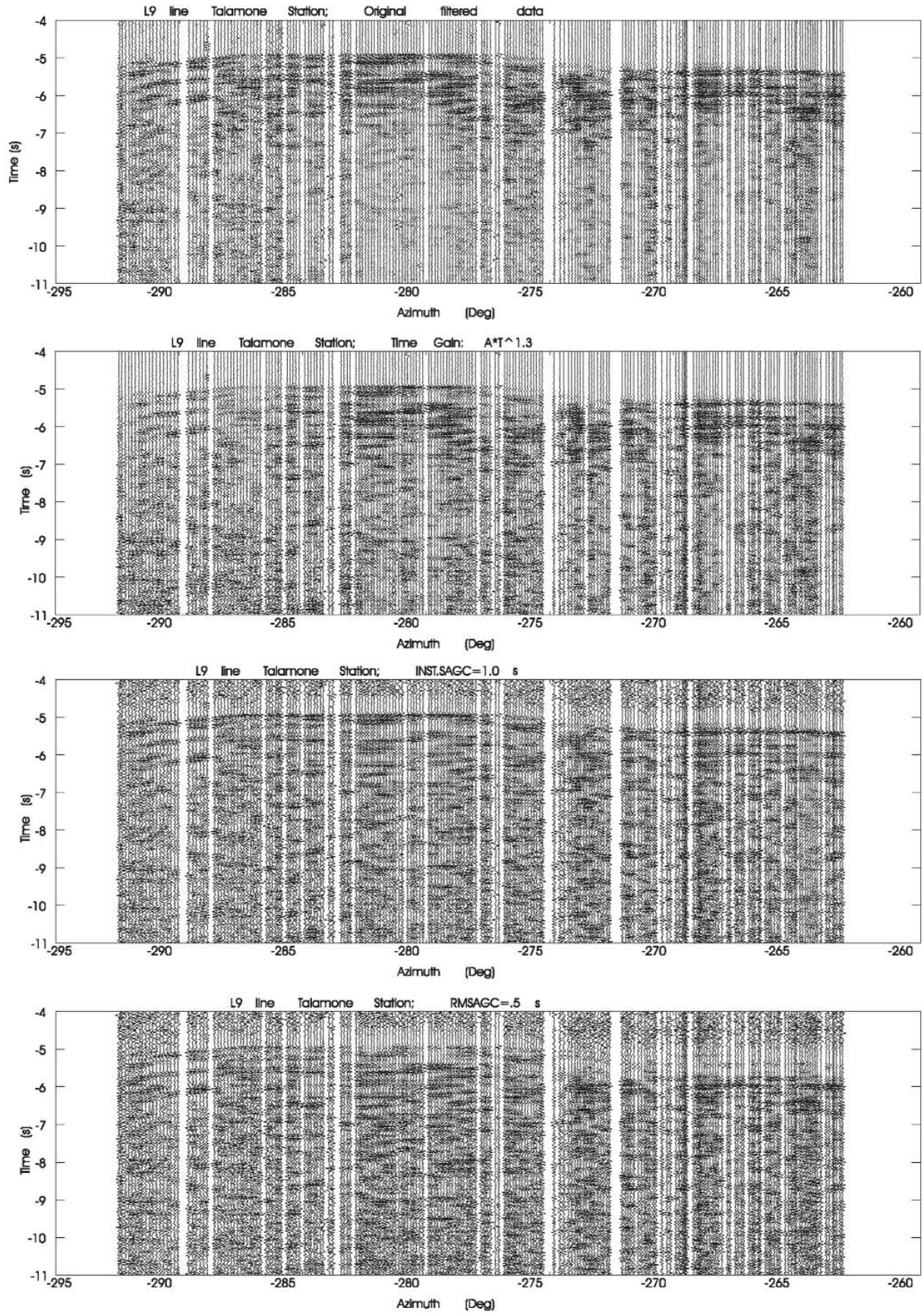

Fig. 4 - Talamone L09 seismic section plotted before and after the application of different gain functions.
- *Sezione sismica Talamone L09 rappresentata prima e dopo l'applicazione di differenti funzioni di guadagno dell'ampiezza.*

in the signal and σ the standard deviation of the coefficients of the highest resolution level.

In some of the seismic sections it was attempted to dampen the T-phase (water wave) by the application of a 2D filter in the frequency-wave number domain (f-k). An example of the filter effect on a CROP MARE II section is shown in figure 5. It was observed that the attenuation of the T-phase over a wide offset range is made difficult by the broadening of the wave train as distance increases, due to the dispersive character of T-wave propagation. Another limitation of 2D-filters derives from the non-constancy of the shot interval, which produces a segmentation of the T-phase.

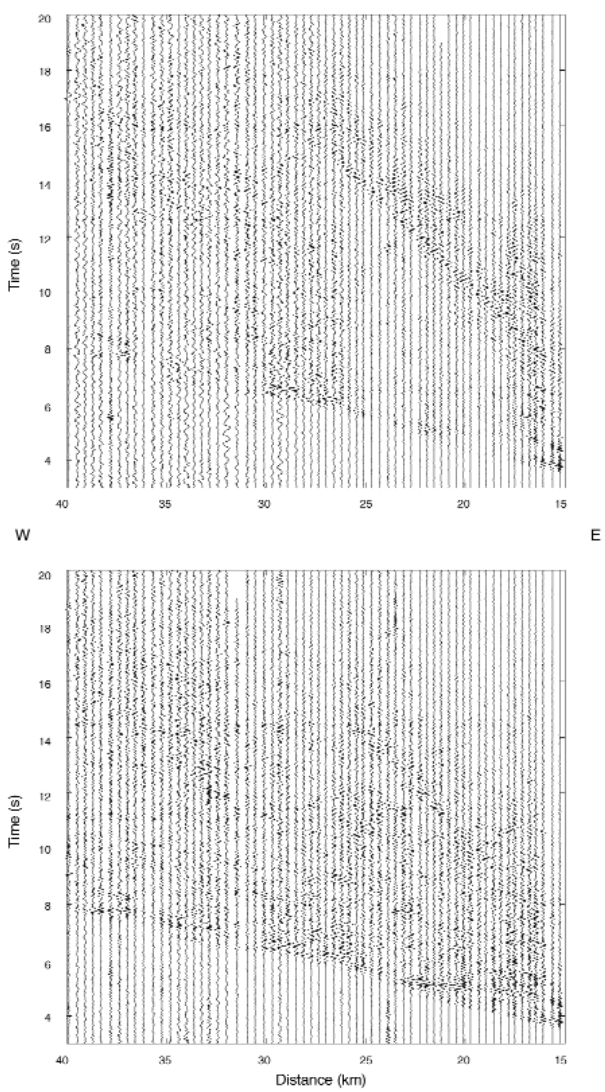

Fig. 5 - Application of the f-k velocity filter: (top) original data; (bottom) data filtered by removing the band – 2 ÷ 2 km/s.

- Applicazione del filtro di velocità f-k: (in alto) dati originali; (in basso) dati filtrati sopprimendo la banda – 2 ÷ 2 km/s.

3.5. - Stacking and trace binning

Stacking is a well-known de-noising technique which is applied nearly always to geophysical measurements typically affected by high-intensity random noise.

In case of high-density wide-angle seismic data, the stacking can be performed between signals originated from a unique seismic source, recorded by small-extension arrays (array stacking), or from several analogous sources at reciprocally close points, recorded by a single station (horizontal binning).

Good-quality results were achieved on the CROP MARE II seismic sections after stacking signals relative to points within a length interval lower than 300 m, both for horizontal binning and for array stacking. The analysis of the effect on binning of varying the length interval (fig. 6) showed that the S/N ratio grows as the number of stacking traces increases, even though for binning radii larger than 450 m the S/N ratio tends to stabilise because of a destructive interference in the signal, but, as the window becomes very wide, horizontal events, certainly interpretable as artefacts, appear in the section (fig. 6c).

For most CROP MARE II sections, having a trace inter-distance about 50 m, the best compromise between increase of S/N and lack of distortions in the processed section was achieved with a window width between 200 m and 400 m.

The binning is made after the equalisation of stacked traces and the application of a space hanning window corresponding to the trace number. After binning, it is suggested to apply a band-pass filter to suppress possible low and high frequencies created by the horizontal stack.

The possibility of using much wider stacking windows obtaining therefore higher S/N ratios was supplied by the MCW algorithm (Chironi *et alii*, 1997). It operates on space-time windows within which the signals are phased by means of a cross-correlation analysis, multiplied by proper weighting factors and stacked. It has been observed that windows up to 800 m wide and even more may be utilised on WARR sections with a trace inter-distance of 50 m without producing significant artefacts. The example shown in figure 7 stresses how the horizontal binning created several artefacts all over the section with a 300-m wide window, whilst no artefacts were produced by MCW despite the more than doubled width of the stacking window, which allowed to achieve a much higher S/N.

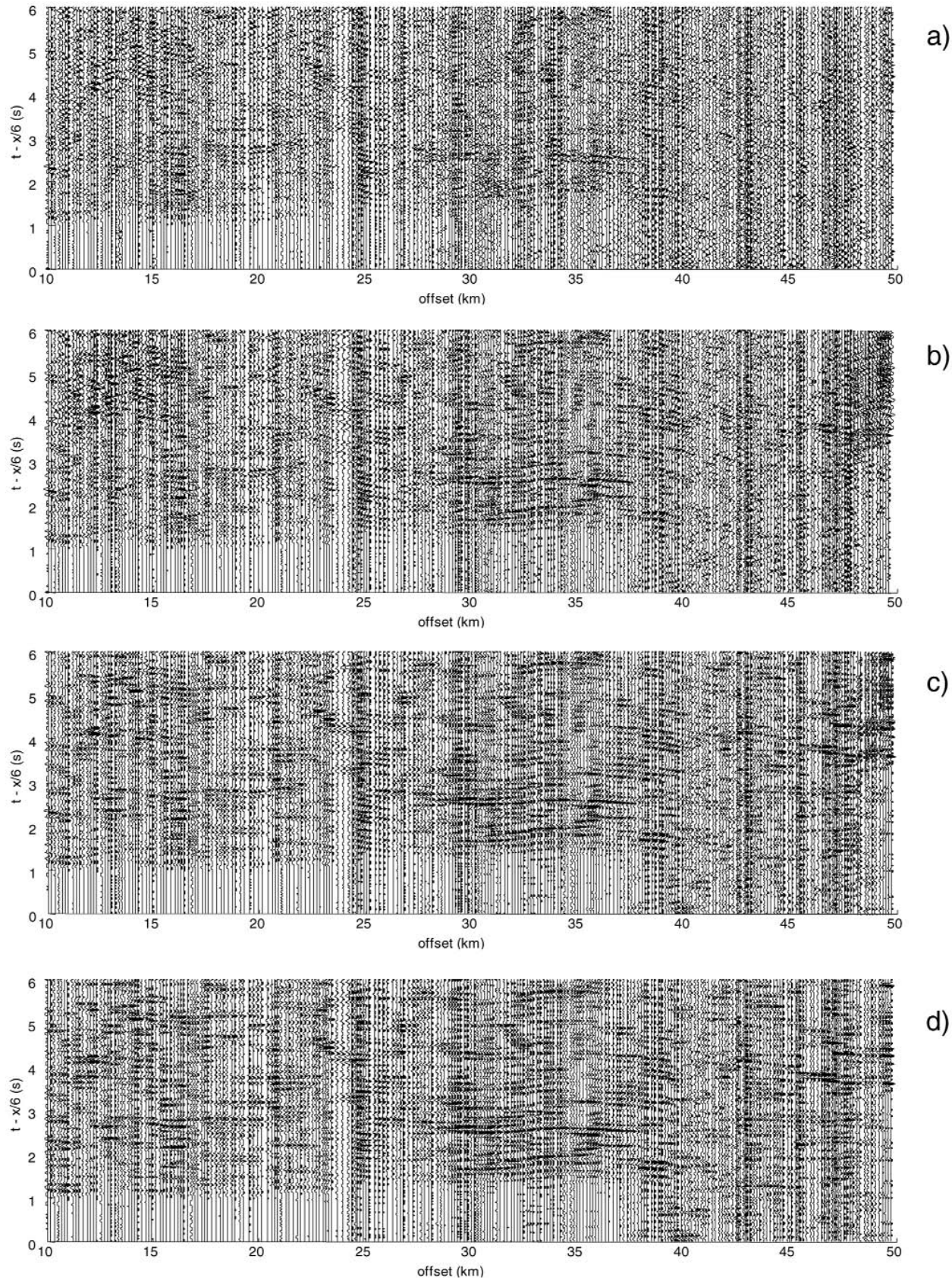

Fig. 6 - Comparison between frequency-filtered data in the band 4-15 Hz: a) without horizontal binning; b) with stacking over 3 traces defining a 300-m wide window; c), with stacking over 5 traces defining a 600-m wide window; d) with stacking over 7 traces defining a 900-m wide window.

- Confronto fra dati elaborati mediante un filtro in frequenza con banda passante 4-15 Hz: a) senza stacking orizzontale; b) con stacking su 3 tracce che definiscono una finestra di 300 m; c) con stacking su 5 tracce che definiscono una finestra di 600 m; d) con stacking su 7 tracce che definiscono una finestra di 900 m.

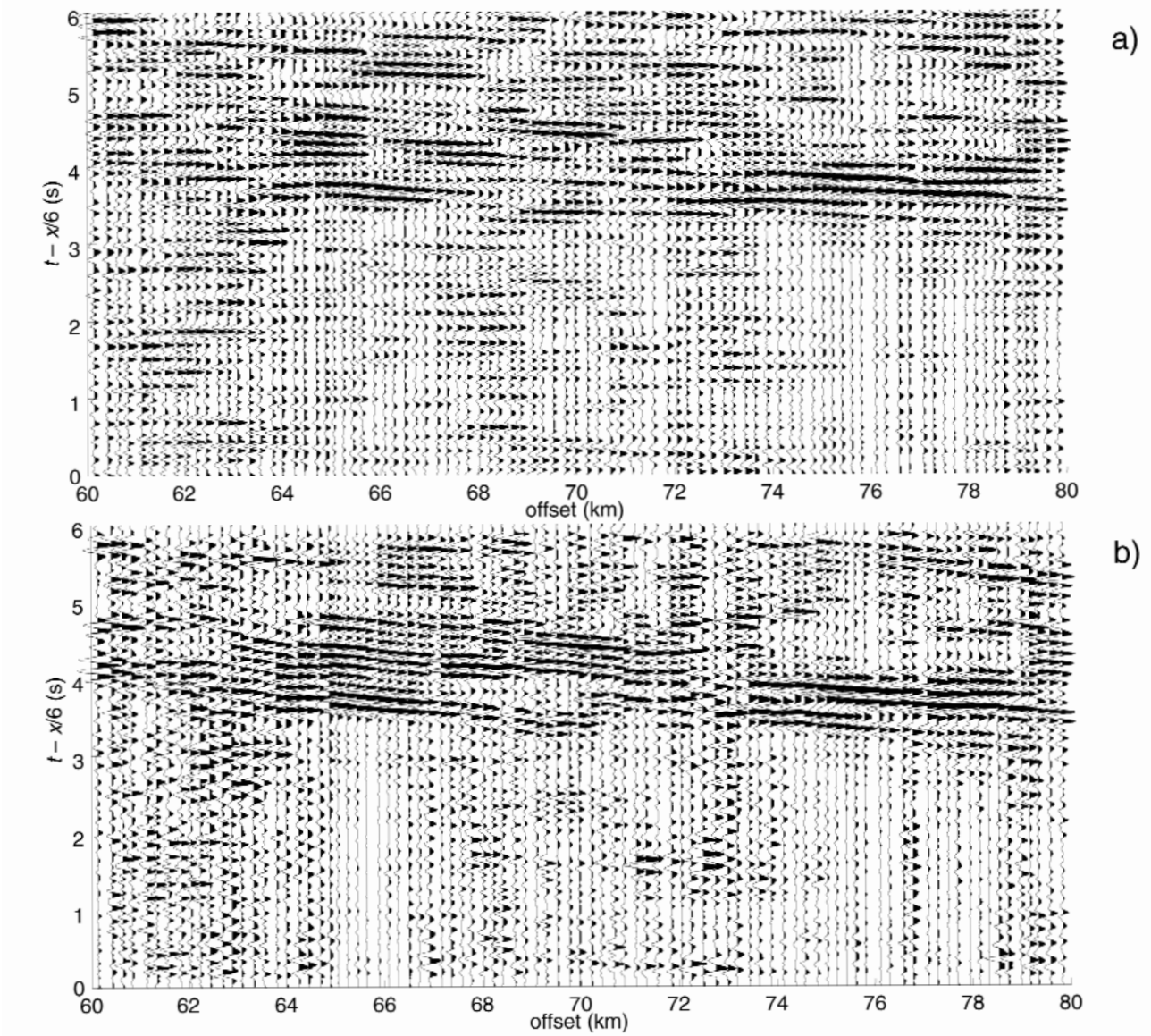

Fig. 7 - Stacking (a) by horizontal binning over 7 traces defining a 300-m wide window and (b) by the MCW algorithm over 15 traces defining a 700-m wide window, applied to a part of the M25 CROP MARE II section.

- Stacking (a) orizzontale su 7 tracce che definiscono una finestra di 300 m e (b) mediante l'algoritmo MCW su 15 tracce che definiscono una finestra di 700 m, eseguito su una porzione della sezione CROP MARE II M25.

An algorithm was also implemented by CHIRONI *et alii* (1997) aimed at a more efficient array stacking in the case of profiles recorded by only 2 stations located in neighbouring sites. It performs a modulation of the stacked section by a weight matrix of equal size obtained with a smoothing of another matrix of coherence attributes calculated on corresponding traces of either original section.

In figure 8a and 8b two corresponding tracts are shown of the sections relative to profile CROP MARE II M28, recorded by stations located on sites 50 m distant from each other. The efficiency of this stacking technique is evident in figure 8c, where the onset of the seismic phase is clearly detectable despite no horizontal binning was applied to the data.

3.6. - COHERENCE FILTERS

Lateral coherence is a wave-field property suitable for constructing de-noising algorithms capable of enhancing phase correlation on WARR seismic sections.

A de-noising algorithm (CDF) was implemented, based on the assumption that on seismic sec-

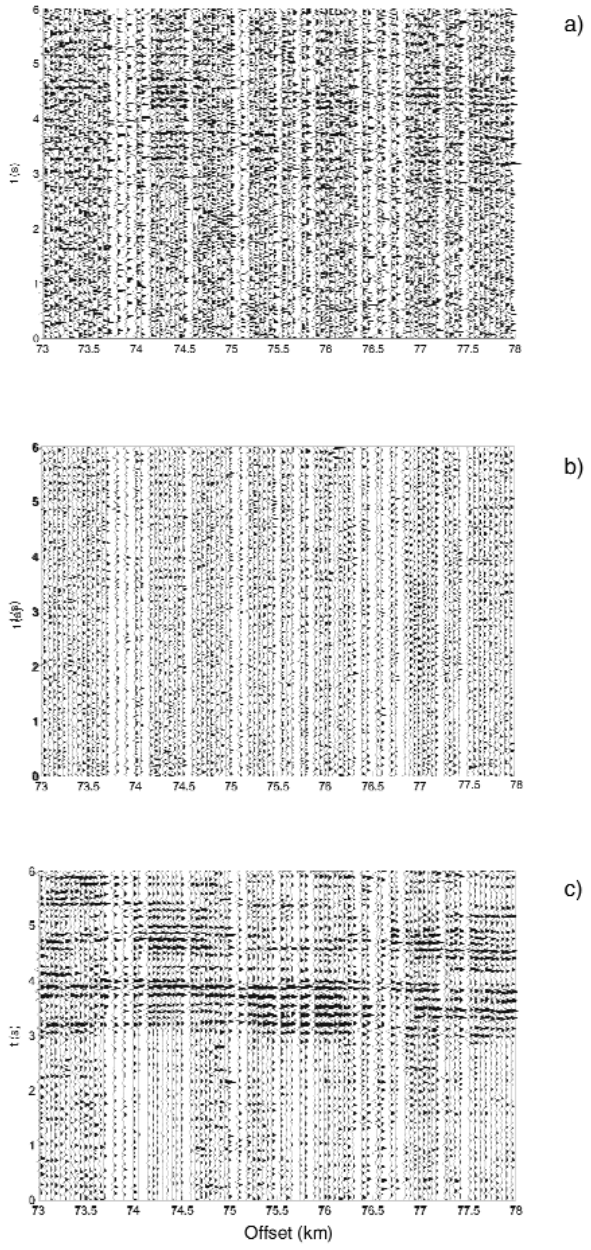

Fig. 8 - (a, b) data relative to profile M28 recorded by two different seismic stations; (c) result of the modulated stacking between the two seismic sections in figure 8a and 8b followed by horizontal binning.

- (a, b) dati relativi al profilo M28 registrato da due diverse stazioni; (c) risultato dello stacking modulato delle due sezioni mostrate in figura 8a e 8b e di un successivo binning orizzontale.

tions signal coherence extends laterally to greater lengths than noise coherence and that the same holds for each detail of a multi-resolution analysis of traces, even though the coherence interval generally becomes narrower as the detail resolution increases.

At first a multi-resolution analysis of traces is executed, followed by a characterisation of space correlation in each multi-resolution detail and the attenuation of the single details in those time intervals in which their lower lateral coherence indicates a lower S/N; finally the de-noised signal is obtained by summing up the attenuated details (Carrozzo *et alii*, 2002).

A quantitative comparison between the results obtained with this de-noising technique and other algorithms (fig. 9) was made by defining suitable indicators of filtering efficiency (Carrozzo *et alii*, 2002).

In figure 9c the result is also shown of a coherence filtering method based on the eigen-image decomposition of seismic sections (Ulrych *et alii*, 1999), so far adopted to process NVR data but also applicable to wide-angle sections within short offset intervals.

3.7. - Polarisation analysis

The acquisition of three-component seismic data makes possible to study the polarisation properties of the wave field. The determination of these properties constitutes an aid to enhance the signal with respect to environmental noise or isolate seismic phases with different polarisation features that cannot be mutually separated with time- or frequency-domain analyses.

The determination of the polarisation attributes of seismic phases may lead to a reliable interpretation of their physical nature, which could not be univocally recognisable by means of amplitudes and travel times.

Some examples of their utilisation in seismic sections modelling and geologic interpretation are the recognition of S- or converted phases and the characterisation of anisotropy at lithospheric or smaller scales (e.g. within shallow layers targeted for oil prospecting).

Some of the authors proposed new polarisation analysis and filtering techniques (De Luca, 2000; De Franco & Musacchio, 2001), since the most widespread ones, designed for the analysis of earthquake data, had proved little effective when applied to crustal wide-angle data, in which numerous phases occur within short time intervals.

In order to evaluate the effectiveness of the new techniques in the processing of this kind of data, they were applied to several CROP MARE II wide-angle seismic profiles.

The algorithm described in De Luca (2000) provides, through the analysis of a cross-energy matrix, estimates of the polarisation vector that prove to be unbiased by the presence of random noise in the case of linearly polarised wave trains.

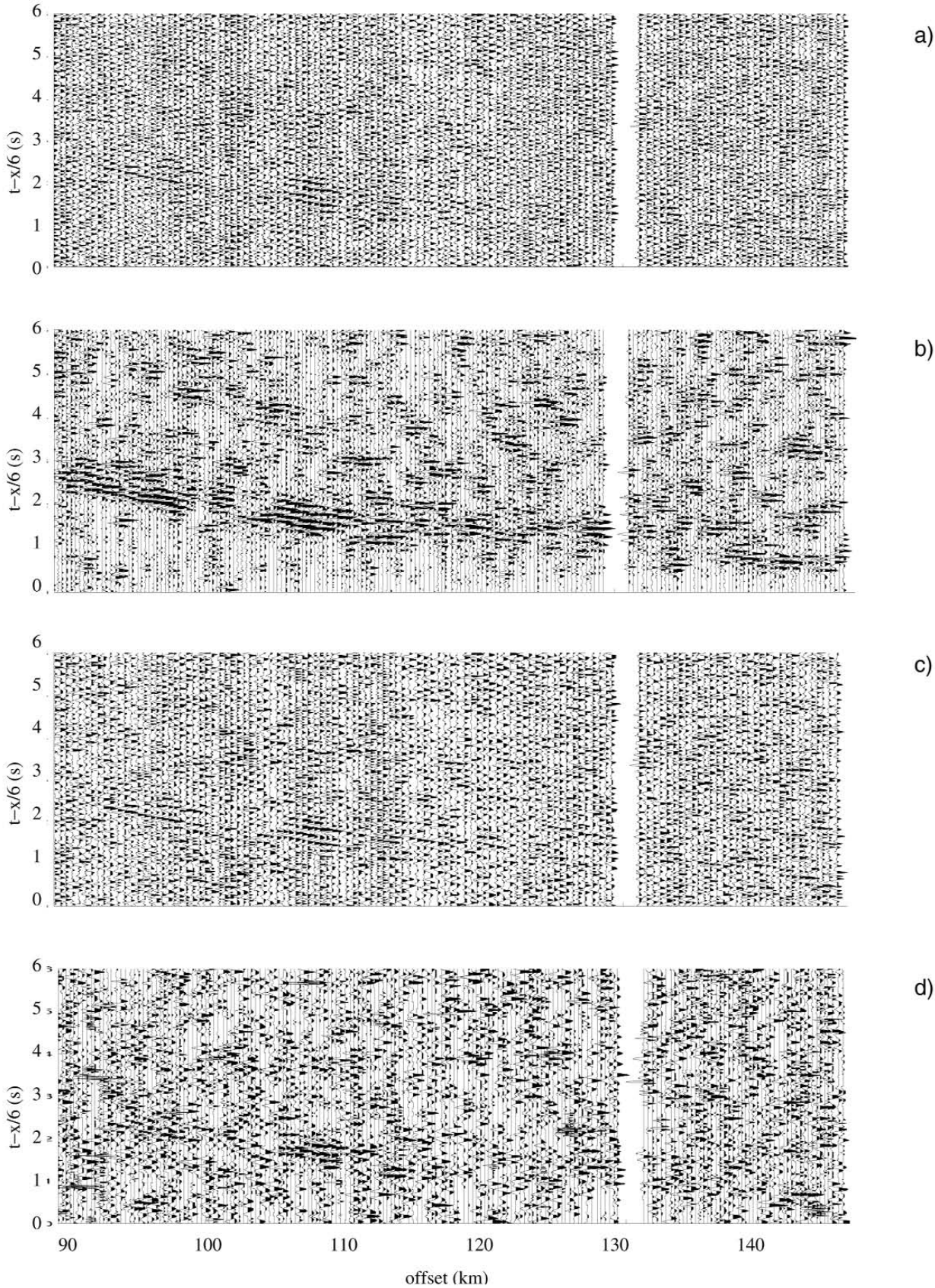

Fig. 9 - Result of the de-noising on the vertical component of the M39 seismic section by (a) Butterworth band-pass filter (5-15 Hz); (b) CDF algorithm; (c) eigenvalue decomposition method; (d) soft-thresholding method.

- Risultato del de-noising sulla componente verticale della sezione sismica M39 mediante (a) un filtro Butterworth nella banda 5-15 Hz; (b) l'algoritmo CDF; c) il metodo delle auto-immagini; (d) il metodo soft-thresholding.

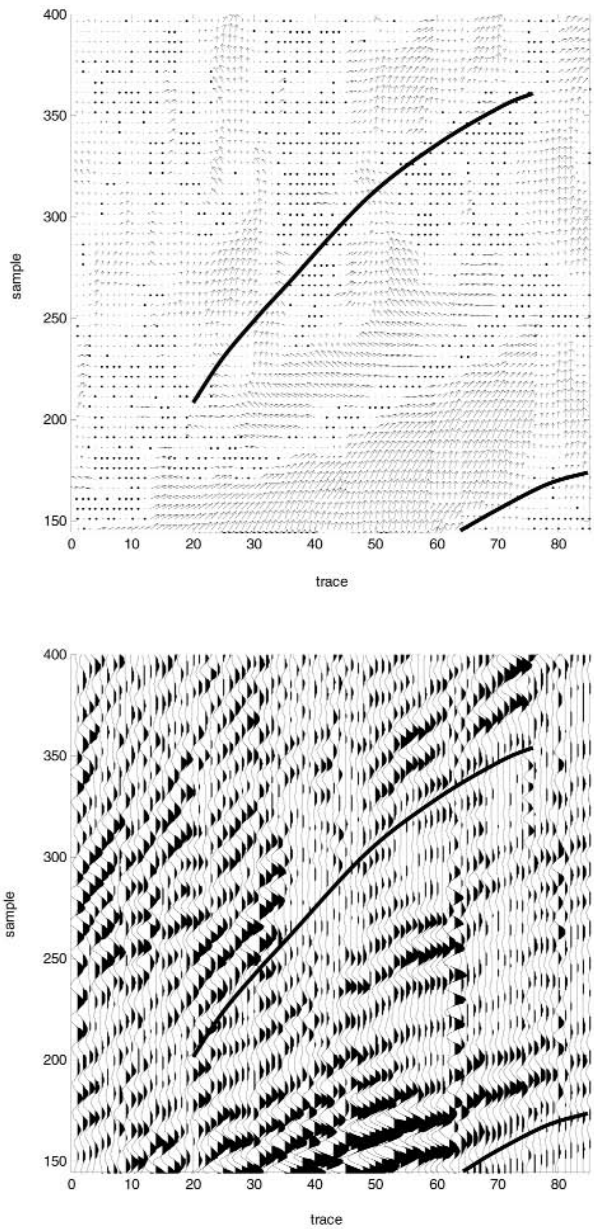

Fig. 10 - Distribution of the polarisation vectors (top) relative to a portion (offset between 17 km and 34 km) of the M27 section (bottom). Their magnitude was modulated with a linearity index.

- Distribuzione dei vettori di polarizzazione (in alto) relativi ad una porzione (offset tra 17 km e 34 km) della sezione M27 (in basso). La loro lunghezza è stata modulata mediante un indice di linearità.

The distribution of these estimates in the M27 section (offsets in the range 17-34 km) is shown in figure 10. In this example the first seismic phase was interpreted as a Pg partially travelling in the sedimentary units of Paola Basin; the delayed phase, which on the basis of its kinematic properties alone had been at first interpreted by some authors of this paper as a P-wave converted to S at the bottom of Paola Basin, was later interpreted (De Luca *et alii*, 2000) by means of the polarisation analysis as a P-wave reflected from the top of the basin and propagating as a diving wave inside it as an effect of the high velocity gradient (fig. 11).

Figure 12 shows some results of an application of a polarisation filter, developed by De Franco & Musacchio (2001) and based on the sum of the first two eigen-images of the singular-value decomposition of a vector seismic trace, to the CROP MARE II M14 profile, in which the filter had enhanced the PmP and SmS phases.

3.8. - Linear and normal move-out transform

These transformations are applied independently to travel times and offsets in order to evidence particular features of the medium seismic responses by their graphical display. Since the transformed time *Ti* is a function of offset *dj* and time, by assuming a constant transformation velocity *Vt* the linear transform is a static correction, whilst the normal-move out transform creates a dynamic distortion of the traces. The first tends to put into evidence the space correlation of pulses, which is characterised by a certain apparent velocity. In this case the transformation or reduction velocity must be close to the apparent velocity of the phases which are to be enhanced. The

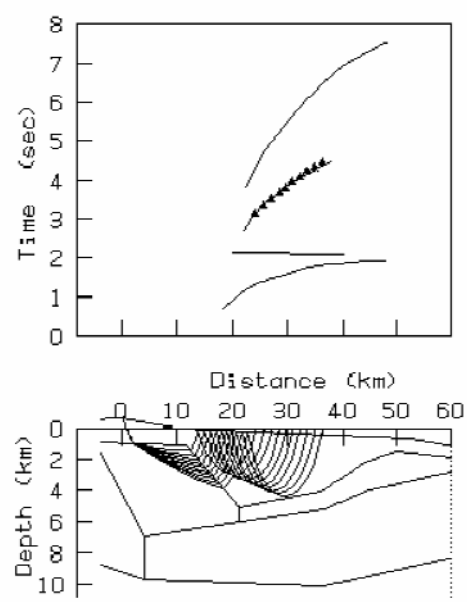

Fig. 11 - Delayed-phase interpretation after polarisation properties analysis.

- Interpretazione della fase ritardata in seguito all'analisi delle proprietà di polarizzazione.

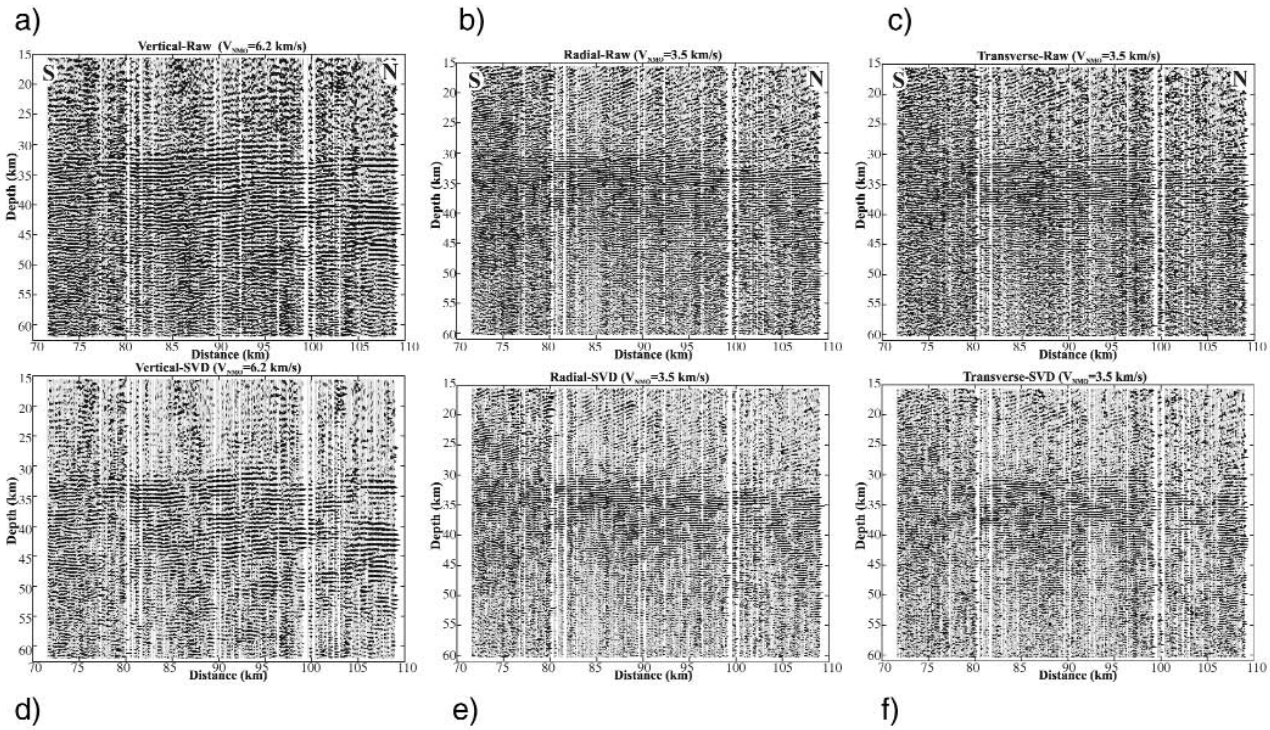

Fig. 12 - Application of the SVD polarisation filter (De Franco & Musacchio, 2001) to M14 CROP MARE II section. The data are displayed in common receiver gather, normalized to maximum amplitude and (Normal Move Out) NMO corrected. NMO correction (V_{NMO} = 6.2 km/s and 3.5 km/s for P- and S-waves, respectively) is applied after the filtering. (a), (b), (c) are the raw data; (d), (e), (f) are the SVD filtered data.

- Applicazione alla sezione sismica CROP MARE II M14 del filtro di polarizzazione basato sulla SVD (De Franco & Musacchio, 2001). I dati sono rappresentati dopo averli normalizzati rispetto all'ampiezza massima e aver effettuato la correzione di Normal Move Out (V_{NMO} = 6.2 km/s and 3.5 km/s per onde P e S rispettivamente). (a), (b), (c) sono i dati originali; (d), (e), (f) sono i dati dopo avere applicato il filtro di polarizzazione.

second transformation modifies each trace so as the pulses relative to a particular reflected phase occur at times next to those of the vertical reflection corresponding to an abscissa equal to half the offset along the profile. In this way these pulses will image the reflector shape. The transformation velocity in this case must represent a good estimate of the root mean square velocity (V_{rms}) of the layers above the reflector.

In both transformations the corrected times are calculated by the formula

$$T_i = \left(t_i^a - \left(d_j / V_i\right)^a\right)^{1/a}, \qquad (5)$$

where a = 1 for linear move-out and a = 2 for normal move-out, j and i are indices referring to the trace and to the time sample. When a = 2, the offset must be transformed with the relation $D_j = d_j/2$.

The use of a V_{rms} depending on time and offset is also possible in order to render an imaging of more boundaries at the same time, but it is more conservative to apply a constant V_{rms} when a reliable information is not available.

Two main problems relative to wide-angle reflection data are still open in normal move-out transformation: 1) NMO transformation should include other corrective terms taking into account the wave refraction effects in a heterogeneous medium, which are not negligible at large offsets; 2) the wide dynamic distortion for large offsets partially eliminable with a re-sampling and filtering.

The NMO-corrected seismic sections relative to the vertical component of all the CROP MARE II lines are reported in an atlas containing the seismic sections relative to vertical component edited by some researchers of the Sea Land group. The V_{rms} was set to 6 km/s in order to achieve a satisfactory imaging of the Moho.

4. - INTERPRETIVE EXAMPLES

In this section some interpretive examples are illustrated, having two principal objectives: the first consists in showing how a suitable processing of WARR data may provide images of the main discontinuities of crustal structures; the second con-

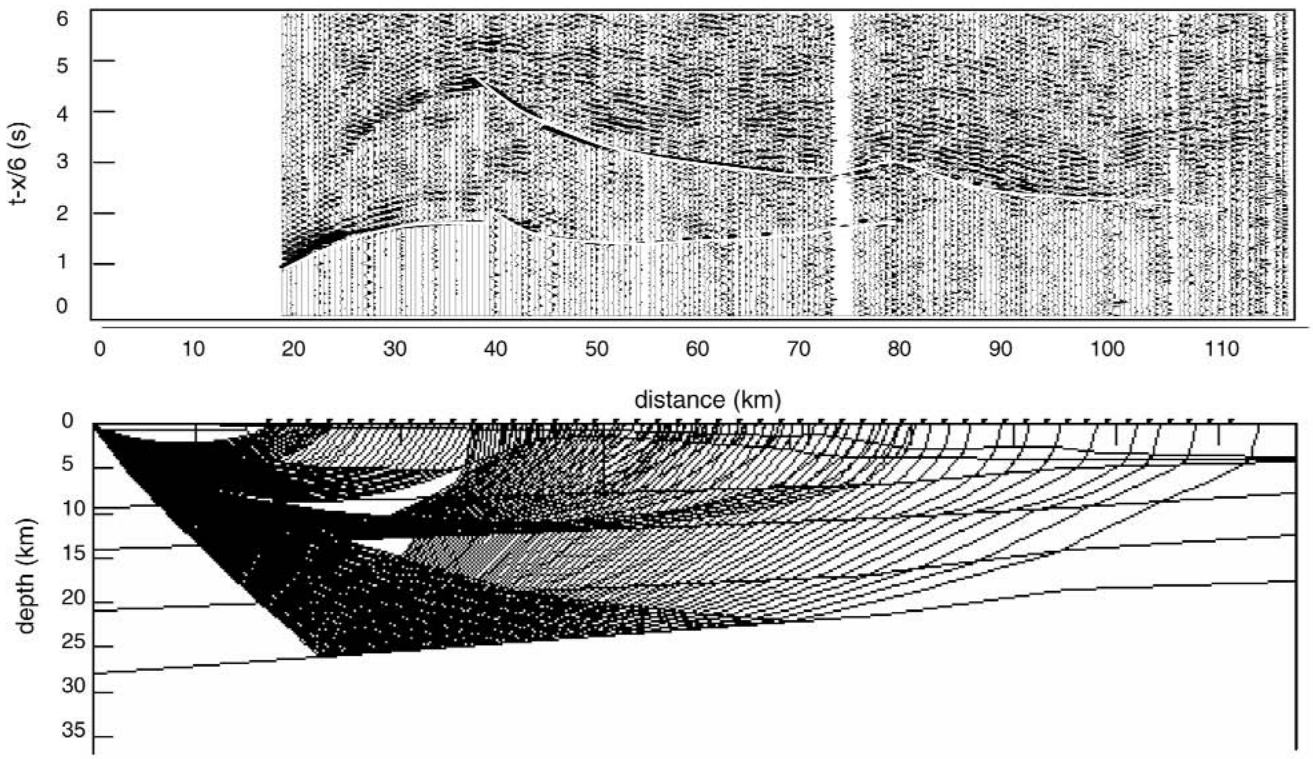

Fig. 13 - Preliminary processing of the M27 CROP MARE II seismic section with superposed calculated travel times (top) and relative ray- tracing (bottom).

- Processing preliminare della sezione sismica CROP MARE II M27 con i tempi teorici sovrapposti (in alto) e relativo ray tracing (in basso).

sists in describing the contribution given by WARR data to NVR data interpretation.

The standard trial-and-error or optimisation inversion techniques for WARR data are mainly based on drawing the travel-times curves of the seismic phases observable on the record sections.

The reliability of the seismic models obtained with these techniques is dependent on the accuracy of travel-time curves and on the degree of confidence on the physical meaning which the corresponding seismic phases are attributed. For this purpose, it appears of primary importance to develop proper enhancing procedures, as stated in the previous sections, the effects of which on the modelling may be viewed in figures 13-14.

The resulting models give a description of crustal structures in terms of smoothed geometric features and average values of the physical parameters which characterise them.

A loss of information with respect to that in the original data is generally observed, due to the averaging processes connected with the smoothing taking place in the phase correlation and with the modelling. A partial retrieval of the details present in the original record sections could be achieved only by a direct imaging performed by suitable transformation of the experimental data. In figure 15 the normal-incidence data section is shown of the Lisa L7 profile, recorded also by Sea Land group in wide-angle configuration. In the same figure a portion is superposed of the NMO-corrected wide-angle section in the offset range where the wide-angle PmP angles are considerably larger than near-vertical reflections. The constant crustal velocity for NMO was optimised according to the ray-tracing model in figure 16.

In order to mark the effect of WARR and NVR integrated imaging, it can be observed that the greater effectiveness of the NVR technique in representing shallow structures can be integrated with the higher capability of WARR data of reconstructing deeper structures.

The imaging using WARR data is a new frontier for data processing, as evinced from the literature. An updated overview is given in Tectonophysics special issues edited by KLEMPERER & MOONEY (1998), where many papers are dedicated to WARR data processing, migration and integration with NVR data.

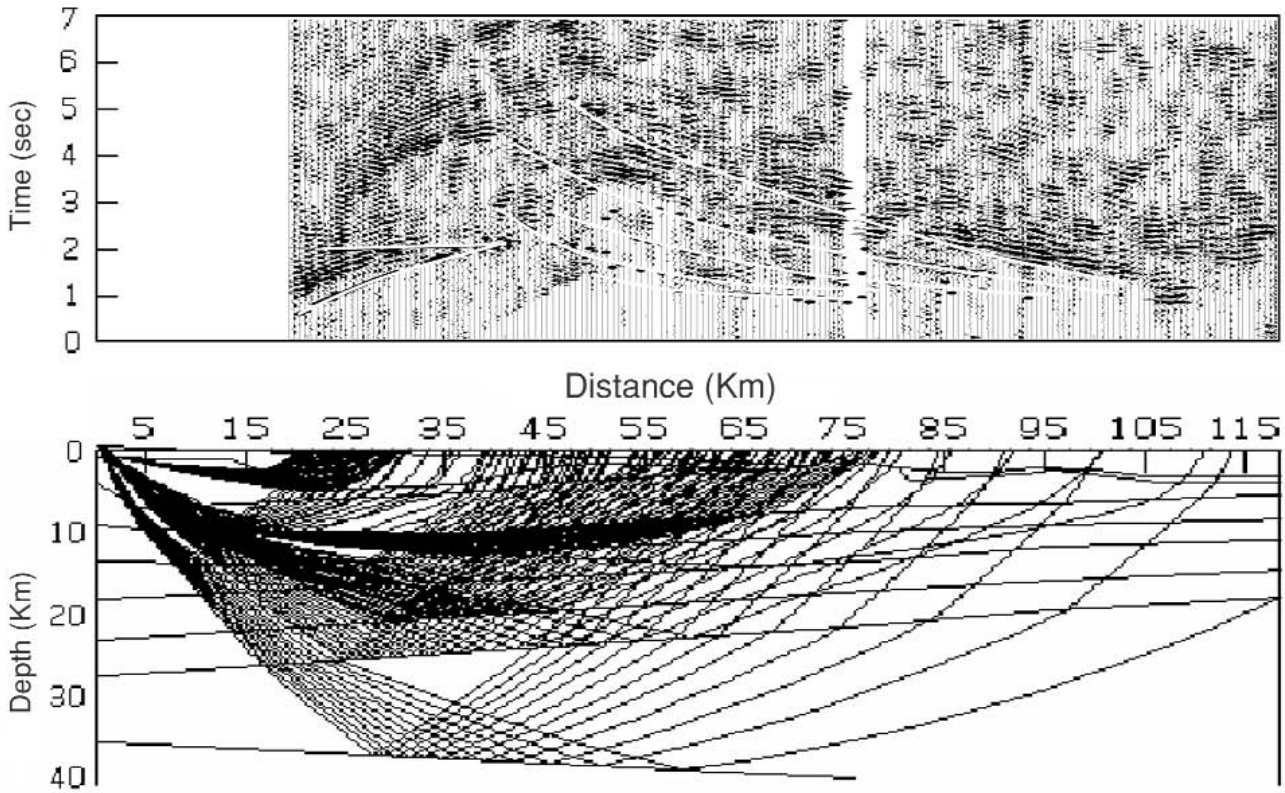

Fig. 14 - Optimised processing of the M27 CROP MARE II seismic section with superposed calculated travel times (top) and relative ray- tracing (bottom).

- Processing ottimizzato della sezione sismica CROP MARE II M27 con i tempi teorici sovrapposti (in alto) e relativo ray tracing (in basso).

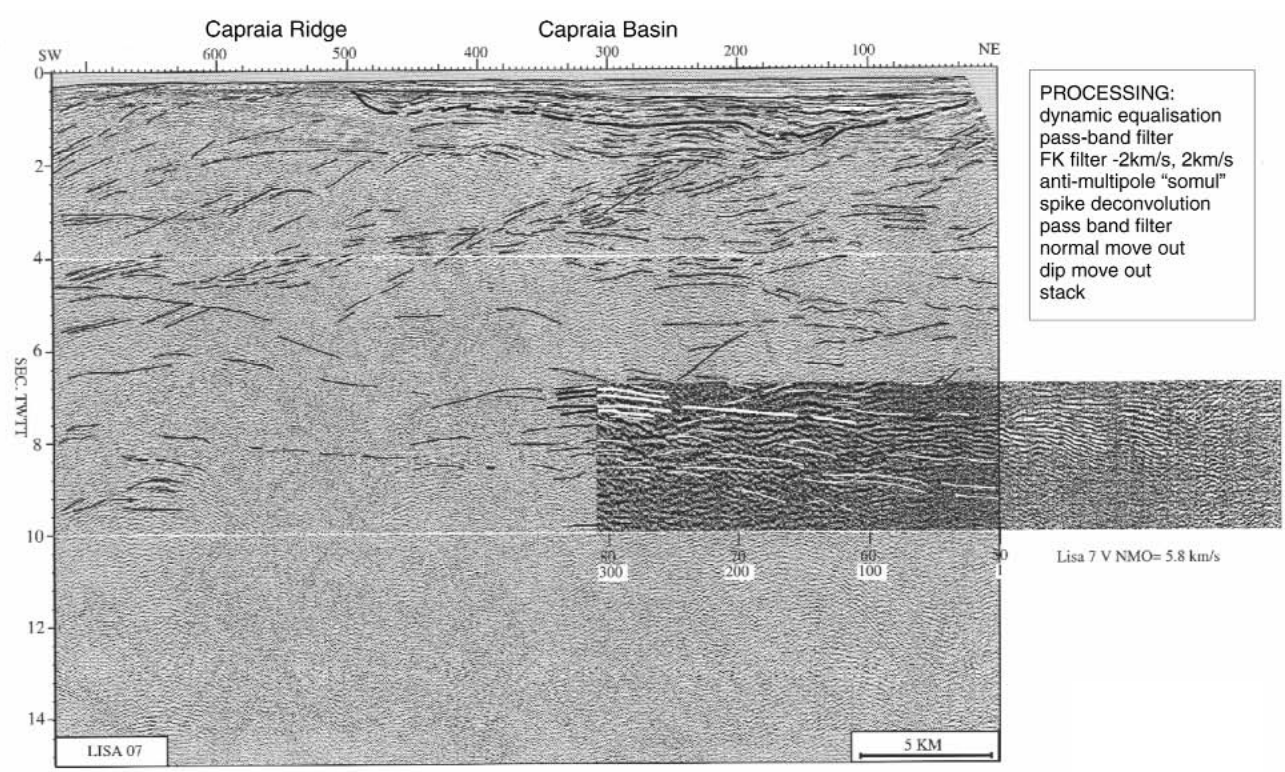

Fig. 15 - Integration between near-vertical data and zero-offset reduced wide-angle data along profile Lisa L7.

- Integrazione di dati near-vertical e dati wide-angle ridotti a offset 0 lungo il profilo Lisa L7.

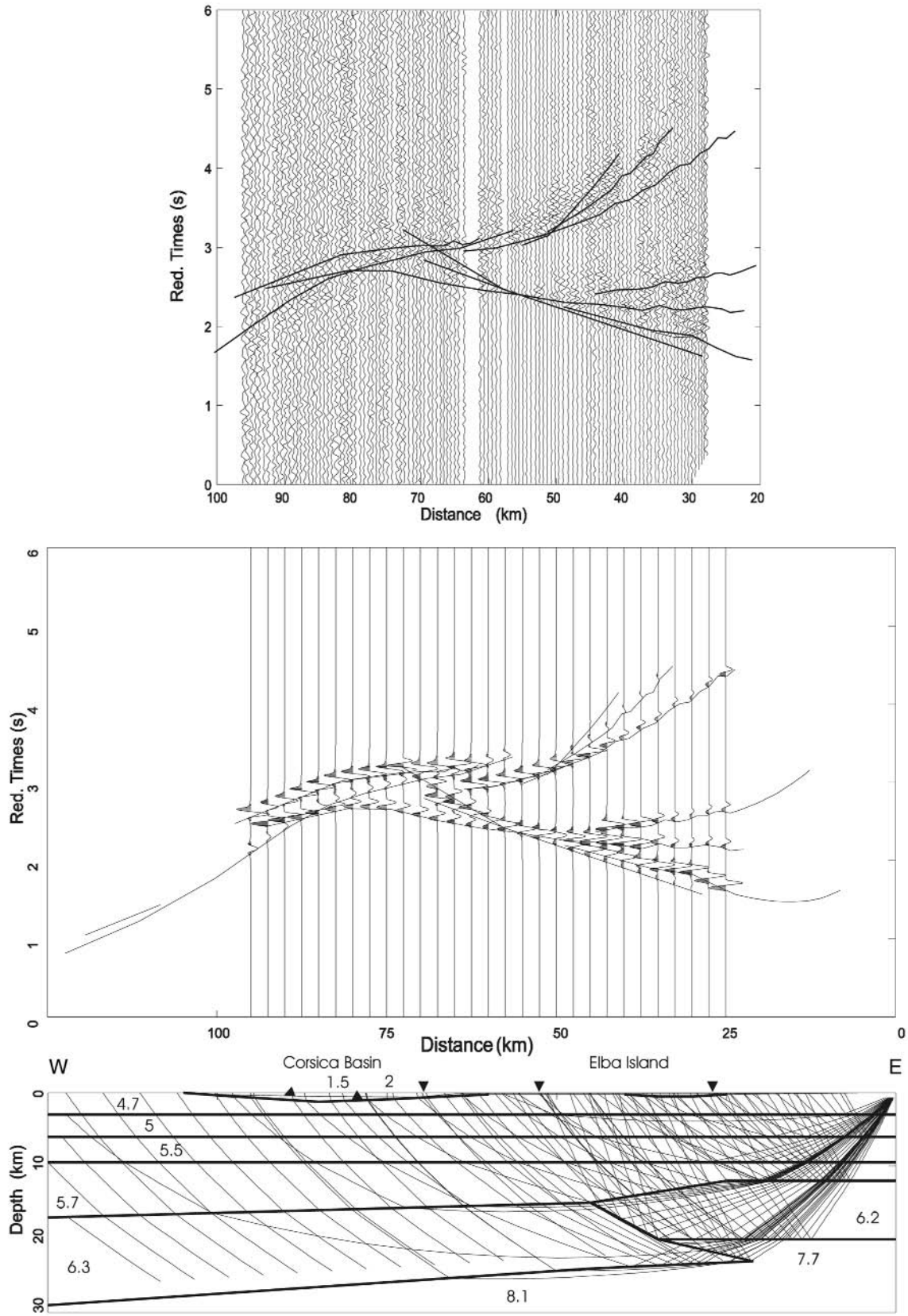

Fig. 16 - Lisa L7 seismic section with superposed calculated travel times (top) and relative ray-tracing (bottom) and synthetic seismo grams (centre).
- Sezione sismica Lisa L7 con i tempi teorici sovrapposti (in alto) e relativo ray tracing (in basso) e sismogrammi sintetici (al centro).

5. - DISCUSSION AND CONCLUSIONS

It was experienced by the researchers of the Sea Land Group that innovative and non-standard processing procedures are necessary for the elaboration of wide-angle reflection/refraction marine data, considering their complex structure. Therefore most of the CROP MARE II seismic sections were processed by a sequence of Matlab-implemented algorithms which, though based on relatively simple concepts, determined a significant increase of the signal-to-noise ratio than that achieved with the application of commercial processing packages, and allowed to provide more informative descriptions of lithospheric structures.

It must be pointed out that the processing algorithms described in the previous paragraphs constitute a tested package, which is flexible both as regards the choice of the parameters involved and the sequence of the algorithms to be applied. For each recorded seismic line an optimal choice of the processing sequence and parameters must be made.

In the forthcoming wide-angle seismic experiments, source choice, data acquisition and data processing constitute the main issues that must be developed, improved and carefully treated during the planning of a survey.

As regards the first one, a crucial matter is the choice of the best station deployment in order to better illuminate off-shore crustal structures and to be able to record data that allow to perform an effective stacking and therefore increase the signal-to-noise ratio.

In designing data acquisition and source characteristics, the following issues should be considered: 1) deployment of OBS for reversed profiling; 2) use of sensor arrays; 3) use of efficient seismic sources; 4) use of a more adequate shooting inter-time; 4) adoption of a large number of active channels (multi-channel/multi-component recording system).

To further improve the survey results, the source and the recording arrays features can be designed for the application of multi-coverage techniques in WARR data analysis.

An important target is the integration of NVR and WARR data in processing and structure imaging. So far the integration has been limited to an exchange of information and constraints between the two techniques. Definitely, this is an important point for which many efforts will be made in the future of seismic data analysis.

REFERENCES

Augliera P., Cattaneo M. & Eva C. (1992) - *Profili sismici wide-angle ad alta risoluzione: prospettive*. Studi Geologici Camerti volume speciale **2** (1992): 35-42.

Babel Working Group (1991) - *Recording marine air gun shots at offset between 300 and 700 km*. Geophys. Res. Letters, **18**, (4): 645-648.

Berry M. J. & Mair J. A. (1980) - *Structure of the continental crust: A reconciliation of seismic reflection and refraction studies*. Spec. Pap. Geol. Assoc. Can., **20**: 195-213.

Braile L. W. & Chiang C. S. (1986) - *The continental Mohorovicic Discontinuity: results from near-vertical and wide-angle seismic reflection studies*. In: M. Barazangi & L. Brown (Eds): *Reflection Seismology: a global perspective*. American Geophysical Union: 257-272.

Carrozzo M.T., De Franco R., De Luca L., Luzio D., Primiceri R., Quarta T. & Vitale M. (2002) - *Wavelet correlation filter for wide-angle seismic data*. Geophysical Prospecting (in press).

Cassinis R. & Lozej A. (2000) - *Targets and peculiarities of "SEA-LAND" wide angle seismic crustal surveys*. Boll. Soc. Geol. It., **119**: 129-140.

Chironi C., De Luca L., Luzio D., Vitale M. & Sea Land Group (1997) - *Algoritmi di stacking per il processing di sezioni sismiche crostali a grande angolo*. Atti 16° Convegno GNGTS, CNR-Roma. CD ROM.

De Franco R., Caielli G., Corsi A. & Group SEA-LAND CROP MARE II (1997) - *Wide angle reflection* SEA-LAND CROP MARE II and LISA *project section atlas*. Convegno Nazionale CROP, 23-24 Jun. 1997, Trieste, Italy.

De Franco R. & Musacchio (2001) – *Polarization filter with singular value decomposition*. Geophysics, **66**, (3): 932-938.

Della Vedova B., Pellis G., Petronio L., Romanelli M., Accaino F., Rinaldi C., Febrer J., Tassone H., Mazzarini F., Bozzo E., Caneva G., Zang J. & Gruppo TENAP (1997) - Progetto TENAP: *indagini crostali attraverso la Penisola Antartica*. Atti 16° Convegno GNGTS. CNR-Roma. CD ROM.

De Luca L. (2000) - *Nuove tecniche di elaborazione ed interpretazione di profili sismici crostali a grande angolo*. PhD thesis, University of Palermo.

De Luca L., Gervasi A., Guerra I., Luzio D., Moretti A. & Vitale M. (2000) - *Elaborazione ed interpretazione dei dati a 3 componenti del profilo M27 (CROP Mare)*. Atti 19° Convegno GNGTS, CNR-Roma. CD ROM.

Donoho D.L. (1995) - D*e-noising by soft-thresholding*. IEEE Trans. Information Theory, **41,** (3): 613-627.

Donoho D. L. & Johnstone I. (1994) - *Ideal spatial adaptation by wavelet shrinkage*. Biometrika, **81**: 425-455.

Gruppo SEA-LAND CROP MARE II (1994) - *Recording of marine airgun shots in peninsular Italy, Sicily and Sardinia* (SEALAND *Project*). Atti 13° Convegno GNGTS, CNR-Roma, 125-131.

Hirn, A., Nicolich, R., Gallart, J., Laigle, M. & Cernobori, L. (1997) - *Roots of Etna volcano in faults of great earthquakes*. Earth Planet. Sci. Letters, **148**: 158-171.

Jokat W. & Fluh E. R. (1987) - *On use of airgun arrays for seismic refraction investigations of the crust*. First Break, **5**, (12): 440-447.

KLEMPERER S.L. & MOONEY W.D. (1998) - *Deep seismic profiling of the continents. General results and new methods*. Tectonophysics, **286**: IX-XIV.

LUND C.E., ROBERTS R.G., JUHLIN C., BODVARSON R. & PALM H. (1987) - *The use of airgun data in crustal reflection-refraction investigations*. Geophys. J. R. astr. Soc., **89**: 365-370.

MAUFFRET A. (1995) - *Scientific report of the LISA Experiment*. Lisa open report file, Lab. de Geotettonique U. Pierre et Marie Curie, Paris.

MEISSNER R., LUESCHEN E. & FLUEH E.R. (1983) - *Studies of the continental crust by near vertical reflection methods: a review*. Phys. Earth and Planet. Interiors, **31**: 363-376.

MJELDE, R., FJELLANGER, J.P., DIGRANES, P., KODAIRA, S., SHIMAMURA, H. & SHIOBARA, H. (1997) - *Application of the Single-Bubble Airgun Technique for OBS-Data Acquisition Across the Jan Mayen Ridge, North Atlantic*. Marine Geophys. Res., **19**: 81-96.

MOONEY W. D. & BROCHER T. M. (1987) - *Coincident seismic reflection/refraction studies of the continental lithosphere: a global review*. Rev. Geophys., **25**, (4): 723-742.

PETRONIO L. (1997) - *Prospezioni sismiche per la valutazione del rischio sismico e vulcanico dell'area etnea e dell'offshore ionico della Sicilia*. PhD thesis, Dipartimento di Ingegneria Navale, del Mare e Ambiente, University of Trieste.

PETRONIO L. & CERNOBORI L. (2000) - *SIMBUS - a seismic source for deep targets and long offset recording*. Boll. Soc. Geol. It., **119**: 159-170.

ULRYCH T., SACCHI M. & FREIRE S. (1999) - *Eigenimage processing of seismic sections*. In: KIRLIN R.L., DONE W.J. & HILL S.S. (Eds.): *"covariance analysis for seismic signal processing"*. Geophys Dev. Series, **8**: 241-274.